HHS Public Access

Author manuscript

Toxicol Appl Pharmacol. Author manuscript; available in PMC 2018 September 15.

Published in final edited form as:

Toxicol Appl Pharmacol. 2017 September 15; 331: 41–53. doi:10.1016/j.taap.2017.05.007.

The expression of keratin 6 is regulated by the activation of the ERK1/2 pathway in arsenite transformed human urothelial cells

Andrea Slusser-Nore, **Scott H. Garrett**, **Xu Dong Zhou**, **Donald A. Sens**, **Mary Ann Sens**, and **Seema Somji***

Department of Pathology, University of North Dakota, School of Medicine and Health Sciences 1301 N. Columbia Road, Stop 9037, Grand Forks, ND 58202

Abstract

Urothelial cancers have an environmental etiological component, and previous studies from our laboratory have shown that arsenite (As^{+3}) can cause the malignant transformation of the immortalized urothelial cells (UROtsa), leading to the expression of keratin 6 (KRT6). The expression of KRT6 in the parent UROtsa cells can be induced by the addition of epidermal growth factor (EGF). Tumors formed by these transformed cells have focal areas of squamous differentiation that express KRT6. The goal of this study was to investigate the mechanism involved in the upregulation of KRT6 in urothelial cancers and to validate that the As^{+3}-transformed UROtsa cells are a model of urothelial cancer. The results obtained showed that the parent and the As^{+3}-transformed UROtsa cells express EGFR which is phosphorylated with the addition of epidermal growth factor (EGF) resulting in an increased expression of KRT6. Inhibition of the extracellular-signal regulated kinases (ERK1/2) pathway by the addition of the mitogen-activated protein kinase kinase 1 (MEK1) and MEK2 kinase inhibitor U0126 resulted in a decrease in the phosphorylation of ERK1/2 and a reduced expression of KRT6. Immunohistochemical analysis of the tumors generated by the As^{+3}-transformed isolates expressed EGFR and tumors formed by two of the transformed isolates expressed the phosphorylated form of EGFR. These results show that the expression of KRT6 is regulated at least in part by the ERK1/2 pathway and that the As^{+3}-transformed human urothelial cells have the potential to serve as a valid model to study urothelial carcinomas.

Keywords

Keratin 6; arsenite; MAPK; bladder cancer; UROtsa; biomarker

*Corresponding Author: Seema Somji, Ph.D., Telephone: 701-777-2658, Fax: 701-777-3108, seema.somji@med.und.edu.

Conflict of interest

The authors declare that they have no competing interests.

1. Introduction

Urothelial carcinoma is the fifth most commonly diagnosed tumor, and among the genitourinary tract malignancies, it is the second most common cause of death in patients from developed countries (Siegel et al., 2013). Urothelial carcinomas are routinely classified into two categories: non-muscle-invasive tumors and muscle-invasive tumors. The 5-year survival for patients with non-muscle-invasive urothelial carcinomas approximates 90%, whereas individuals with muscle-invasive tumors have 5-year survival frequencies of approximately 60% (Luke et al., 2010). Individuals with non-muscle-invasive disease appear to have a high rate of recurrence, and some with recurrence are found to have progressed to muscle-invasive disease (Zuiverloon et al., 2012). There are few effective chemotherapeutic treatment options for patients with muscle-invasive disease, illustrating the need for new prognostic markers to identify and further study those early lesions prone to progress to a more invasive disease status. One marker that appears to have prognostic utility for urothelial carcinomas is squamous differentiation of the urothelial cancer cells, but a major drawback is that its appearance appears very late in disease progression. While urothelial carcinomas that contain a prominent squamous component are rare, there is evidence that the presence of a squamous component indicates a poor prognosis for the patient. Focal squamous differentiation has been shown to be an unfavorable prognostic feature for patients undergoing radical cystectomy (Frazier et al., 1993) or radiation therapy (Martin et al., 1989; Akdas and Turkeri, 1990) and is associated with a poor response to systemic chemotherapy (Logothetis et al., 1989). Recently, molecular profiling has shown that muscle invasive bladder cancer can be grouped into basal and luminal subtypes similar to what has been seen in breast cancers (Choi et al., 2014). Basal muscle invasive bladder cancers are enriched with squamous features with elevated expression of epithelial keratins (KRT) such as KRT5, KRT6 and KRT14 in addition to other basal genes as seen in breast cancers (Perou et al., 2000).

This laboratory has previously published data indicating that the expression of KRT6 might be developed as a marker that can detect early squamous differentiation of urothelial carcinomas before it is readily visible by diagnostic microscopy. In these studies, it was shown using the immortalized, but not tumorigenic, human urothelial cell line, that malignant transformation of the cells by both arsenite (As^{+3}) and cadmium (Cd^{+2}) resulted in tumor transplants where expression of KRT6 was co-localized to areas of overt squamous differentiation (Rossi et al., 2001; Sens et al., 2004; Somji et al., 2008; Cao et al., 2010; Somji et al., 2011). In these studies, 6 independently isolated As^{+3}-transformed cells and 7 independently isolated Cd^{+2}-transformed cells were used, and all produced tumor transplants where KRT6 expression was co-localized to areas of overt squamous differentiation. It was also shown using a small subset of archival specimens of human urothelial carcinomas that KRT6 staining could identify small, focal areas of squamous differentiation in some urothelial carcinomas that might be missed on routine microscopic examination (Somji et al. 2008).

The goal of the present study was two-fold. One, to further validate that the As^{+3}-transformed UROtsa cells are a good model that retains important characteristic features of urothelial cancer. To achieve this goal, the expression of the epidermal growth factor

receptor (EGFR) and the activation of the EGFR signaling pathway was determined in the parental as well as the As^{+3}-transformed UROtsa cells, and their tumor transplants. The rationale for this examination is that it is well documented that the EGFR pathway is frequently overexpressed in human urothelial cancer and overexpression correlates with higher tumor grade/stage and poorer prognosis (Neal et al., 1990; Miyamoto et al., 2000; Izumi et al., 2012; Mooso et al., 2015). The demonstration of expression of the EGFR pathway in the As^{+3}-transformed cells would also reinforce the known role of arsenic exposure in the etiology of urothelial cancer. The second goal was to determine the mechanism leading to the increased expression of KTR6 in As^{+3}-transformed UROtsa cells and their derived tumor transplants. Specifically, to determine if expression of keratin 6 expression is influenced by the EGFR pathway and if this might further define its potential for development as an early biomarker of adverse prognosis.

2. Materials and Methods

2.1. Animals

Mouse heterotransplants of the UROtsa transformed cell cultures were produced by subcutaneous injection at a dose of 1×10^6 cells in the dorsal thoracic midline of athymic nude (NCR-*nu/nu*) mice. Tumor formation and growth were assessed externally with a ruler on a weekly basis and the maximal tumor size was 2.5 cm. All mice were sacrificed by 10 weeks after injection or when clinical conditions dictated euthanasia (excessive weight loss, lethargy, self-mutilation or mutilation by cage mates). This study adhered to all recommendation dictated in the Guide for the Care and Use of Laboratory Animals of the NIH. The specific protocol was approved by the University of North Dakota Animal Care Committee (IACUC#1110-2C). All efforts were taken in order to minimize animal suffering, and mice were euthanized when clinical condition dictated. Animals were sacrificed by 10 weeks post tumor transplantatio n by CO_2 inhalation and euthanasia conformed to American Veterinary Medical Association Guideline on Euthanasia.

2.2 Cell culture

The UROtsa parent cells and the six independent As^{+3}-transformed isolates were cultured in 75 cm^2 tissue culture flasks in Dulbeco's modified Eagle's medium (DMEM) supplemented with 5% vol/vol fetal bovine serum as described previously (Rossi et al., 2001; Sens et al., 2004). Since the As^{+3}-transformed cells have not been cloned, they are being referred to as isolates in the study. The cells were subcultured at a 1:4 ratio using trypsin-EDTA and the cultures were fed fresh growth medium every three days. To determine the effects of epidermal growth factor (EGF), the cells were grown to confluency in 25 cm^2 flasks as described above. At confluence, EGF (10ng/ml) was added to the cells for various time periods and the cells were harvested.

2.3 Real-Time analysis of KRT 6A mRNA expression

Keratin 6a mRNA expression was assessed with real-time reverse transcription polymerase chain reaction (RT-PCR) using primers that were developed using Oligo 6.0 software. The sequences of the upper and lower primer of KRT6A along with the product sizes are as follows: sense: CTAAAGTGCGTCTGCTA antisense: TGGGTGCTCAGATGGTATA

(product size, 184 bp). Total RNA was purified from the cells lines and 0.1 μg was subjected to cDNA synthesis using the iScript cDNA synthesis kit (Bio-Rad Laboratories, Hercules, CA) in a total volume of 20 μL. Real-time RT-PCR was performed using the SYBR Green kit (Bio-Rad Laboratories) with 2 μL cDNA and 0.2 μM primers in a total volume of 20 μL in an iCycler iQ real-time detection system (Bio-Rad Laboratories). Amplification was monitored by SYBR Green fluorescence. Cycling parameters consisted of denaturation at 95°C for 15 sec, annealing at 55°C for 45 sec, and extension at 72°C, which gave optimal amplification efficiency. The levels of keratin 6a were determined by serial standards. The resulting levels were normalized to the change in β-actin expression assessed by the same assay using the primers, sense: CGACAACGGCTCCGGCATGT and antisense: TGCCGTGCTCGATGGGGTACT, giving a product size of 194 base pairs and with the cycling parameters of annealing/extension at 62°C for 45 s and denaturation at 95°C for 15 s.

2.4 Western blot analysis

Cells were rinsed twice with cold phosphate - buffered saline and were incubated with 1X Radio-immunoassay Precipitation Assay (RIPA) lysis buffer supplemented with PMSF, protease inhibitor cocktail and sodium orthovandate (Santa Cruz Biotechnology, Dallas, TX) for 5 min on ice. Following incubation, the cells were scrapped and transferred to a conical tube. The cell suspension was sonicated and the lysate was centrifuged to remove cellular debris. The protein concentration was determined using the bicinchoninic protein assay (Pierce Chemical Co, Rockford, IL). Total cellular protein (20 μg) was separated on a 12.5% SDS-polyacrylamide electrophoresis gel and transferred to a hybond-P polyvinylidene difluoride membrane (Amersham Biosciences, Piscataway, NJ). Membranes were blocked in Tris-buffered saline (TBS) containing 0.1% Tween-20 (TBS-T) and 5% (wt/vol) nonfat dry milk for 1 h at room temperature. After blocking, the membranes were probed overnight with the primary antibody diluted in buffer containing 5% bovine serum albumin. The primary antibodies against KRT6 was purchased from Santa Cruz Biotechnology (Santa Cruz, CA) whereas the antibody against β-actin was purchased from Abcam Inc. (Cambridge, MA). The KRT6 antibody does not distinguish between the isoforms and recognizes proteins made by the KRT6A, KRT6B and KRT6C genes. Hence, the protein is referred to as KRT6 in the manuscript. The antibodies against EGFR, p-EGFR, Extracellular Signal-Regulated Kinases 1 and 2 (ERK1/2), p-ERK1/2, c-Jun N-terminal kinase (JNK), p-JNK, AKT serine/theonine kinase (AKT) and p-AKT were purchased from Cell Signaling Technology (Beverly, MA). After incubation with the primary antibody, the blots were washed 3 times with TBS-T, and the membranes were incubated with the anti-mouse or anti-rabbit secondary antibody (1:2000) for 1 h. The blots were visualized using the Phototope-HRP Western blot detection system (Cell Signaling Technology).

2.5 Determination of MAPK activation by EGF in UROtsa parent and transformed cells

UROtsa parent and transformed cells were grown to confluence in serum containing medium, following which the cells were incubated with DMEM without serum for 24 h. The cells were then exposed to 10 ng/ml EGF for 1, 4, 8, 12 and 24 h and were harvested for Western blot analysis.

2.6 Treatment of cells with the MEK1/2 inhibitor U0126

UROtsa parent cells and the As^{+3}-transformed cell line, As#4 were grown to confluence in serum containing medium following which the cells were incubated with DMEM without serum for 24 h. Following serum deprivation, the cells were pretreated for 2 h either with 10 μM U0126 (Cell Signaling Technology) dissolved in dimethyl sulfoxide (DMSO) or they were treated with DMSO alone. After 2 h, the cells were treated with EGF (10ng/ml) and DMSO or they were treated with EGF and the inhibitor U0126. The cells were harvested in RIPA lysis buffer after 1, 4, 8, 12 and 24 h of treatment.

2.7 Immunostaining for EGFR and pEGFR in tumor transplants

Tumor tissue from mouse tumor transplants was routinely fixed in 10% neutral-buffered formalin for 16–18 h. The fixed tissue samples were transferred to 70% ethanol and dehydrated in 100% ethanol. The dehydrated tissue samples were cleared in xylene, infiltrated, and embedded in paraffin. Serial sections were cut at 3–5 μm for use in immunohistochemical protocols. Prior to immunostaining, sections were immersed in preheated Target Retrieval Solution (Dako, Carpinteria, CA) and heated in a steamer for 20 min. The sections were allowed to cool to room temperature and immersed into TBS-T for 5 min. The EGFR antibody was used at a dilution of 1:100, whereas the pEGFR antibody was used at a dilution of 1:200. The primary antibodies were localized using Dako peroxidase conjugated EnVision plus for Rabbit Primary Antibodies at room temperature for 30 min. Liquid diaminobenzidine (Dako) was used for visualization. Counter staining was performed for 8 min at room temperature using Ready-to-use Hematoxylin (Dako). Slides were rinsed with distilled water, dehydrated in graded ethanol, cleared in xylene, and coverslipped.

2.8 Statistics

Statistical analysis consisted of ANOVA with Tukey *post-hoc* testing performed by Graphpad PRISM 4. All experiments were done in triplicates and the data is plotted as the mean ± SEM of triplicate determinations.

3. Results

3.1 Expression of KRT6 in the UROtsa parent and As^{+3}-transformed cells

The basal expression levels of KRT6A mRNA and KRT6 protein were determined in the UROtsa parent and the As^{+3}-transformed cells by real-time PCR and Western blot analysis. KRT6 has three isoforms encoded by three closely linked genes on chromosome 12. With amino acid sequence identity of about 98%, it is not possible to develop isoform-specific antibodies. The individual isoforms can be measured at the mRNA level with PCR. Each gene has only one transcript capable of encoding a protein, albeit there are several intron-retaining alternatively spliced variants. The primer pairs developed to measure each isoform are specific for the protein-encoding transcript of each KRT6 isoform. Previously we had shown that the KRT6A isoform is the predominant isoform that is expressed in the UROtsa parent and the As^{+3}-transformed isolates. In addition, we also showed that the expression KRT6B was very low and KRT6C was not expressed in the UROtsa parent or the As^{+3}-transformed isolates (Cao et al. 2010). We therefore determined the expression of KRT6A

isoform in all the UROtsa cells. As shown in Fig. 1, the expression level of KRT6A was low in the UROtsa parent cells whereas the expression level was variable in the As^{+3}-transformed cells. There was a significant increase in expression of KRT6A in As#1, As#2, As#3, As#4 and As#6, when compared to the UROtsa parent cells as shown in Fig. 1A, B and C. The expression level of KRT6A in As#5 was similar to the level seen in the UROtsa parent cells. Since the antibody used for Western analysis recognizes total KRT6 protein due to sequence homology between the KRT6 isoforms, therefore protein levels from the individual genes cannot be assessed.

3.2 Effect of EGF on the expression of KRT6 in the UROtsa parent cell line and the As^{+3}-transformed UROtsa isolates

Previous studies from our laboratory have shown that EGF can induce the expression of keratin 6 (Somji et al., 2008). In the present study, the UROtsa parent cells and the As^{+3}-transformed isolates were treated with 10 ng/ml of EGF for 1, 4, 8, 12 and 24 h and Western analysis was performed on the cell lysates. The results showed that the expression level of KRT6 was low in the UROtsa parent cells; however, treatment with EGF significantly increased the expression of KRT6 (Fig. 2A and B) by 12 h and it remained elevated at 24 h. This suggests that EGF can induce the expression of KRT6 in the UROtsa parental cells. In all the six As^{+3}-transformed UROtsa isolates, there was basal expression of KRT6 (Fig. 3). Addition of EGF increased the expression of KRT6 in As#1 (Fig. 3A), As#2 (Fig. 3B), As#3 (Fig. 3C) and As#4 (Fig. 3D) isolates by 12 h, however there was no increase in the expression in As#5 (Fig. 3E) after the addition of EGF. For As#6, there was an increase in KRT6 expression only after 24 h of exposure (Fig. 3F).

3.3 Effect of EGF on the activation of the EGFR and downstream kinases in the UROtsa parent cell line and As^{+3}-transformed UROtsa isolates

Since binding of EGF to its receptor on cell surfaces results in the phosphorylation of the receptor and activation of various signal transduction pathways (Kyriakis et al., 2001), we assessed the activation of EGFR, ERK1/2, c-Jun N-terminal kinases (JNK1/2) and AKT serine/theonine kinase (AKT) in the UROtsa parent cells and the As^{+3}-transformed isolates. As shown in Fig. 2 and Fig 4 (A – F), the UROtsa parent and the As^{+3}-transformed isolates expressed EGFR. Addition of EGF to the UROtsa parent cells resulted in in the phosphorylation of EGFR by 1 h, following which the levels started to decrease by 4 h and returned to basal levels by 8 h (Fig. 2A and C). For the transformed isolates, addition of EGF resulted in the phosphorylation of the receptor after 1 h of exposure in all the isolates and the levels of phosphorylation decreased to basal levels by 4 h of exposure. However, in As#2 (Fig. 4B), the level of phosphorylation decreased by 4 h and by 12 h, there was an increase in phosphorylation which remained elevated till 24 h of treatment indicating a biphasic activation of the EGFR in this isolate.

In the UROtsa parent cells, there was activation of the ERK signaling pathway after 1 h of EGF exposure and the levels of the phosphorylated form started to decrease by 4 h and reached basal levels at 24 h of exposure (Fig. 2A and D). Addition of EGF to the As^{+3}-transformed isolates resulted in the phosphorylation of ERK1/2 in all the transformed isolates, however the pattern of phosphorylation varied (Fig. 5). In As#1 (Fig. 5A), there was

phosphorylation after 1 h of treatment following which the phosphorylation levels started to decrease by 4 h and returned to basal levels by 12 h of treatment. In As#2 (Fig. 5B), As#4 (Fig. 5D), As#5 (Fig. 5E) and As#6 (Fig. 5F), there was an increase in phosphorylation after 1 h of treatment, following which the levels decreased but at later time points, it increased again showing a biphasic pattern of activation. In As#3 (Fig. 5C), the level of phosphorylation increased after 1 h of treatment following which it decreased and returned to basal level for the rest of the time course.

The JNK1/2 pathway was also activated in the UROtsa parent cells after 1 h of exposure to EGF, but it decreased to basal levels at 2 h (Fig. 2A and E). For the As^{+3}-transformed isolates, activation of JNK1/2 following EGF treatment was only seen in As#1 (Fig. 6A) and As#3 (Fig. 6C), whereas in As#2 (Fig. 6B), As#4 (Fig. 6D), As#5 (Fig. 6E) and As#6 (Fig. 6F), there was no phosphorylation of JNK1/2. In As#1 (Fig. 6A), there was low levels of phosphorylation after 1 h of EGF treatment and it went down to basal levels at 4 h. In As#3 (Fig. 6C), JNK1/2 was phosphorylated after 1 h of treatment and the levels went down by 4 h, however there was increased phosphorylation at 24 h showing a biphasic pattern of activation.

The AKT pathway was also activated after 1 h of exposure in the UROtsa parent cells and returned to basal levels by 24 h of exposure (Fig. 2A and E). AKT (Fig. 7) was phosphorylated in all the As^{+3}-transformed isolates except As#4 (Fig. 7D), which did not show any phosphorylation. In As#1 (Fig. 7A), As#2 (Fig. 7B), As#5 (Fig. 7E) and As#6 (Fig. 7F), there was phosphorylation after 1 h of exposure following which the levels decreased but remained elevated compared to the untreated controls. In As#3, AKT was phosphorylated following 1 h of treatment following which the levels decreased to basal levels during rest of the time course.

3.4 Effect of mitogen-activated protein kinase kinase 1/2 (MEK1/2) Inhibitor U0126 on the expression KRT6 in the UROtsa Parent and As^{+3}-Transformed Cell Line

To determine if the activated ERK1/2 pathway influenced the expression of KRT6, the parent UROtsa cells and the As#4 cell line that expressed elevated levels of KRT6 when compared to the UROtsa parent cells were treated with the MEK1 and 2 kinases (ERK kinases) inhibitor U0126. Both the isolates were pretreated with the U0126 inhibitor or DMSO (vehicle control) for 2 h, followed by the addition of 10 ng/ml EGF or 10 ng/ml of EGF and 10 μM U0126 for 1, 4, 8, 12 and 24 h. The dose of the inhibitor that was used is according to the instructions provided by the manufacturer (Cell Signaling Technology). There was no toxicity to the cells with this dose of U0126 (data not shown). Treatment of the parental cell line with EGF resulted in an increase in expression of KRT6 when compared to the untreated cells (Fig. 8A and 8B). However, when the inhibitor was added, there was a decrease in expression of KRT6 when compared to cells treated with EGF alone (Fig 8A and B). Following 12 h of exposure of the parental UROtsa cells to EGF plus U0126, the expression of KRT6 was reduced to near basal levels of expression. Treatment of the cells with the inhibitor and EGF also reduced the levels of the phosphorylated form of ERK1/2 when compared to the cells treated only with EGF (Fig 8A and C). Treatment of the As^{+3}-transformed isolate (As#4) with the inhibitor also resulted in a decrease in the levels of

KRT6 when compared to EGF treated cells and non-treated cells (control) as shown in Fig. 9A and B. The phosphorylation of ERK1/2 was also decreased in the presence of U0126 (Fig. 9A and C). There was no effect of the inhibitor on total ERK1/2 in the UROtsa parent (Fig. 8A and C) or the As#4 isolate (Fig. 9A and C).

3.5 Immuno-histochemical localization of EGFR and pEGFR in As^{+3}-transformed subcutaneous tumor transplants

This laboratory has shown previously using immuno-histochemistry that tumor transplants from all 6 independently generated As^{+3}-transformed isolates expressed KRT6, even though one of the isolates lacked *in vitro* expression of KRT6 (Cao et al., 2010). The present examination was designed to determine if the *in vitro* data showing the presence of EGFR is translated to the *in vivo* tumor transplants including any evidence of EGFR activation in the *in vivo* tumor cells. Immuno-histochemical staining showed that all tumor transplants derived from the 6 independently generated As^{+3}-transformed UROtsa isolates stained intensely for EGFR (Fig. 10A, C, E, G, I and K). The staining was localized to the cell membrane of the tumor cells and staining was most intense at the periphery of the tumor nests and less intense or absent in the center of the nests. Immunohistochemisty demonstrated that only 2 of the 6 tumor transplants (Fig. 10B and D) showed staining for the phosphorylated form of EGFR, and when present the staining was focal and localized to the cell membrane. The intensity and staining pattern for EGFR and pEGFR in the tumor transplants generated from the As^{+3}-transformed isolates is summarized in Table 1.

4. Discussion

The first goal of the present study was to determine if the As^{+3}-induced malignant transformation of the UROtsa cell line produced tumor transplants that possessed important features of human urothelial carcinoma. The initial characterization of tumor transplants produced from subcutaneous injection of the As^{+3}-transformed UROtsa cells showed a histology consistent with human urothelial carcinoma or what was commonly referred to in past nomenclature as transitional cell carcinoma (Sens et al., 2004; Somji et al., 2008; Cao et al., 2010; Somji et al., 2011). However, other markers characteristic of human urothelial carcinomas were not assessed in this model system. In the present study, the parental UROtsa cell line, the As^{+3}-transformed isolates, and tumor transplants generated from the As^{+3}-transformed isolates were assessed for their expression of EGFR. The results demonstrated that the parental UROtsa cells and the As^{+3}-transformed isolates and resultant tumor transplants all expressed high basal levels of the EGFR. This is an important validation of this model system from several perspectives. First, in normal human urothelium, EGFR is expressed in the basal layer and correlates with a less differentiated state of these cells (Messing et al., 2012). This provides evidence that the parental UROtsa cells are derived from the basal layer of the normal urothelium and that the As^{+3}-transformed isolates and tumors retain the basal undifferentiated state characteristic of cancer. Second, the finding that the As^{+3}-transformed isolates and resultant tumor transplants expressed high levels of EGFR is consistent with the observation that overexpression of EGFR is frequently found in human urothelial carcinoma. As summarized by Mooso and co-workers (Mooso et al., 2015), EGFR is frequently overexpressed in human

urothelial carcinoma and overexpression is more common and occurs more frequently in muscle-invasive urothelial carcinoma that in non-muscle-invasive disease. There are several studies that have shown that overexpression of EGFR in muscle invasive urothelial cancer is associated with higher tumor stage, increased tumor progression and poor clinical outcome (Mellon et al., 1995; Colquhoun and Mellon, 2002). Thus, our data demonstrates that the UROtsa cells malignantly transformed by As^{+3} are showing an important feature of human urothelial carcinoma that is associated with an aggressive form of the disease. An interesting finding that should be mentioned is that the tumors derived from the As^{+3}-transformed isolates showed strong staining in approximately 50% of the tumor cells. The reason for this is unknown but could be due to tumor heterogeneity or simply that EGFR expression is transient depending on the proliferative state of the tumor cell. Thus, the As^{+3}-transformed UROtsa cells and derived tumor transplants retain an important feature of human urothelial carcinoma.

The present study also demonstrated that the EGFR signaling pathway could be activated by the addition of EGF in the parental UROtsa cells and the As^{+3}-transformed isolates. It was shown that the addition of EGF resulted in the phosphorylation of EGFR and the activation of the principle members of the mitogen-activated protein kinase (MAPK) family; ERK1/2 (p-ERK1/2) and JNK1/2 (p-JNK1/2). In addition, there was also activation of the AKT (p-AKT) in the cells after the addition of EGF. The pattern of phosphorylation of EGFR varied among the UROtsa cells and the transformed isolates. The finding that the UROtsa cell line and the transformed isolates retains an active EGFR signaling pathway is important since studies in human urothelial carcinoma have suggested that the EGFR pathway plays a critical role in cell proliferation, differentiation, migration, angiogenesis and apoptosis (Bellmunt et al., 2003; Black et al., 2007; MacLane et al., 2008). The activation of the ERK1/2 signaling pathway was also varied with a transient increase in phosphorylation followed by a decrease in some of the isolates whereas in others, there was a sustained increase in phosphorylation throughout the time course, and some showed a biphasic pattern of activation. Activation of JNK was limited and was only seen in the UROtsa parent, As#1 and As#3 isolates. The activation pattern also varied with the parent and As#1 showing phosphorylation after 1 h of exposure with return to basal levels by 4 h and As#3 showing a biphasic pattern of activation. Since we only looked at activation after 1 h of exposure, it is possible that JNK was phosphorylated in the other isolates within minutes of exposure to EGF and it returned to basal levels by 1 h of exposure. AKT is also known to be activated by EGF (Joo et al., 2016), and we determined the activation of this pathway. The pattern of activation was variable and similar to what was seen for the ERK1/2 signaling pathway. One of the isolates, As#4 did not show activation of AKT after exposure to EGF. Biphasic activation of signaling pathways has been reported previously and this has been observed in colorectal cancer cells that were stimulated with EGF (Joo et al., 2016). In this study, EGF was removed from the culture media and there was reactivation of the ERK1/2 pathway without further exposure to EGF. However, the distribution pattern of pERK1/2 was different suggesting a different role of pERK1/2 during reactivation. Previously, global gene expression analysis of all of the As^{+3}-transformed isolates have shown a high degree of heterogeneity of gene expression with hundreds to well over a thousand genes that are differentially expressed between the isolates (Garrett et al., 2014). It is, thus, conceivable

that there is variation in the expression level of components of the EGF signaling pathway as well as other pathways that may cross-talk with this pathway. Tumors in general are well known to exhibit a high degree of heterogeneity due to genomic instability (Gerlinger, et al, 2012; Gerlinger et al., 2015) and the As^{+3}-transformed UROtsa cell isolates are thus a good model of tumor heterogeneity. It is expected that a similar level of variation in response to EGF would exist in human bladder cancers. This varied pattern could also influence the progression of the disease and resistance to therapeutic agents. Lastly, the immunohistochemical analysis of the arsenite tumor transplants for pEGFR indicated that the EGF receptor is autophosphorylated in two of the six As^{+3}-transplants suggesting that the EGR receptor is currently active and engaged in cellular signaling. Our experiments *in-vitro* with the isolates showed that the phosphorylation of the EGF receptor correlated to the activation of the MAP kinase pathway, and thus, it is reasonable to assume that this pathway is active in the tumor heterotransplants. Overall, these finding support the concept that the UROtsa cell line can provide a valuable model to study As^{+3}-induced urothelial carcinoma. The UROtsa model provides a platform to study the acute toxicity of As^{+3} in the parental non-malignant cell line, the subsequent *in-vitro* transformation of the parental cells by chronic As^{+3} exposure, and the *in vivo* tumor biology of the transformed isolates when transplanted into immune compromised mice. The ability to study both the acute and chronic effects of As^{+3} exposure in one human bladder cell line is important. This is because As^{+3} exposure, in addition to causing acute toxicity to the bladder, has a well-established strong association for the development of human urothelial carcinoma with chronic exposure (Cantor and Lubin, 2007; Chiou et al., 1995, Luster and Simeonova, 2004; Smith et al., 1998; Steinmaus et al., 2000; Tsuda, et al., 1995).

The final goal of the study was to determine the mechanism involved in the expression of KRT6 in the parental and As^{+3}-transformed UROtsa isolates. The results showed that the level of KRT6 was low in the UROtsa parent and one of the As^{+3}-transformed isolate As#5. Addition of EGF increased the expression of KRT6 in the UROtsa parent cells. The effect of EGF on the expression level of KRT6 was varied in the As^{+3}-transformed isolates with some of the isolates showing significant increase in expression of KRT6, whereas in other there was very little or no effect on the expression of KRT6. In one of the isolates As#5 that expressed very low levels of KRT6, addition of EGF had no effect. These variations in the responses of each of the metal-transformed isolate to EGF and the expression of KRT6 is to be expected since there is variation in the expression of various genes in these transformed isolates.

The increased expression of KRT6 protein by the addition of EGF in the UROtsa parental as well as one of the As^{+3}-transformed isolates, As#4 was inhibited by treating the cells with the ERK1/2 inhibitor, U0126. These results show that the expression of KRT6 in both the parental and As^{+3}-transformed UROtsa cells is regulated by the ERK1/2 pathway. The MEK inhibitor U0126 was chosen for this study as it has been shown to attenuate the activity of the transcription factor AP-1 (Duncia et al., 1998) which has been implicated in the upregulation of KRT6 expression (Ma, et al., 1997). Since As#4 showed a decrease in the levels of KRT6 protein levels, when compared to the control untreated cells after treatment with the inhibitor U0126, this suggests that the activation of the ERK1/2 pathway plays a major role in regulating the expression of KRT6 in As^{+3}-transformed cells. However, the

participation of other signaling pathways in regulating the expression of KRT6 cannot be ruled out and needs further investigation.

The interest in KRT6 as a possible biomarker for urothelial cancer arose from the laboratory's previous studies on KRT6 expression in the As^{+3}- and Cd^{+2}-transformed tumor transplants and a sample set of archival specimens of human urothelial carcinoma (Somji et al., 2008; Cao et al., 2010; Somji et al., 2011). In these studies, it was shown that KRT6 expression correlated to areas of overt focal squamous differentiation in subcutaneous transplants of the As^{+3}- and Cd^{+2}-transformed urothelial cells. The finding that rendered this correlation of interest to biomarker development was that peritoneal tumor transplants from some of these same isolates expressed much less focal squamous differentiation and KRT6 staining was able to highlight and identify these much less notable areas of squamous differentiation. A similar finding was found in a small archival set of formalin-fixed, paraffin-embedded patient specimens where KRT6 staining was able to identify small areas of squamous differentiation. These findings, taken together, suggested that identification of very early steps in the process of squamous differentiation in urothelial cancer could have prognostic significance. Currently, large areas of focal squamous differentiation are easily identifiable by routine diagnostic pathology of hematoxylin and eosin stained slides and other antibody markers have also been identified that will stain larger regions of focal squamous differentiation (Fong et al., 2003; Lopez-Beltran et al., 2009; Hayashi et al., 2011; Huang et al., 2013). In contrast, KRT6 staining was able to identify small areas of squamous differentiation before they were easily detectable by microscopic examination. It is possible that early identification of squamous differentiation would increase the ability to predict aggressive tumors since squamous features have been linked to aggressive behavior of bladder cancers (Kim et al., 2012; Mitra et al., 2013). A potential problem with the continued development of KRT6 as an early biomarker for squamous differentiation is that the keratins are a very large family of proteins with significant overlap in sequence among the family members (Moll et al., 2008). This presents a problem in studies using immunohistochemistry on large patient-derived samples of diagnostic material, where antibody specificity cannot be determined for the individual samples. It would be likely that due to the large amount of tumor heterogeneity that other keratins might be expressed that would cross-react with KRT6 in large archival studies thus complicating interpretation of the results. Thus, understanding the mechanism controlling KRT6 expression might identify other molecular markers that would decrease the probability of cross-reactivity for evaluation of early squamous differentiation in urothelial carcinoma.

Acknowledgments

The research described was supported by funds provided by the Department of Pathology and the School of Medicine and Health Sciences, University of North Dakota. Undergraduate research, graduate student mentoring, core facilities for bioinformatics, statistics, and gene expression were supported by the ND INBRE IDeA program P20 GM103442 from the National Institute of General Medical Sciences, NIH.

Abbreviations

AKT	AKT serine/threonine kinase
As^{+3}	arsenite

Cd^{+2}	cadmium
DMEM	Dulbecco's modified Eagle's medium
DMSO	dimethyl sulfoxide
EGF	epidermal growth factor
EGFR	epidermal growth factor receptor
ERK	extra-cellular signal regulated kinases
JNK	c-Jun N-terminal kinase
KRT	keratin
MEK	mitogen-activated protein kinase kinase 1
RIPA	radioimmunoprecipitation assay
TBS	Tris-buffered saline
TBS-T	Tris-buffered saline with Tween-20

References

Akdas A, Turkeri L. The impact of squamous metaplasia in transitional cell carcinoma of the bladder. Int J Urol Nephrol. 1990; 23:333–336.

Bellmunt J, Hussain M, Dinney CP. Novel approaches with targeted therapies in bladder cancer. Crit Rev Oncol Hematol. 2003; 46:85–104.

Black PC, Agarwal PK, Dinney CP. Targeted therapies in bladder cancer - an update. Urol Oncol. 2007; 25:433–438. [PubMed: 17826665]

Cantor KP, Lubin JH. Arsenic, internal cancers, and issues in inference from studies at low-level exposures in human populations. Toxicol Appl Pharmacol. 2007; 222:252–257. [PubMed: 17382983]

Cao L, Zhou XD, Sens MA, Garrett SH, Zheng Y, Dunlevy JR, Sens DA, Somji S. Keratin 6 expression correlates to areas of squamous differentiation in multiple independent isolates of As^{+3}-induced bladder cancer. J Appl Toxicol. 2010; 30:416–430. [PubMed: 20186695]

Chiou HY, Hsueh Y, Liaw KF, Hong SF, Chiang MH, Pu YS, Lin JS, Huang CH, Chen CJ. Incidence of internal cancers and ingested inorganic arsenic: a 7-year follow-up study in Taiwan. Cancer Res. 1995; 55:1296–1300. [PubMed: 7882325]

Choi W, Porten S, Kim S, Willis D, Plimack ER, Hoffman-Censits J, Roth B, Cheng T, Tran M, Lee IL, Melquist J, Bondaruk J, Majewski T, Zhang S, Pretzsch S, Baggerly K, Siefker-Radtke A, Czerniak B, Dinney CP, McConkey DJ. Identification of distinct basal and luminal subtypes of muscle-invasive bladder cancer with different sensitivities to frontline chemotherapy. Cancer Cell. 2014; 25:152–165. [PubMed: 24525232]

Colquhoun AJ, Mellon JK. Epidermal growth factor receptor and bladder cancer. Postgrad Med J. 2002; 78:584–589. [PubMed: 12415079]

Duncia JV, Santella JB 3rd, Higley CA, Pitts WJ, Wityak J, Frietze WE, Rankin FW, Sun JH, Earl RA, Tabaka AC, Teleha CA, Blom KF, Favata MF, Manos EJ, Daulerio AJ, Stradley DA, Horiuchi K, Copeland RA, Scherle PA, Trzaskos JM, Magolda RL, Trainor GL, Wexler RR, Hobbs FW, Olson RE. MEK inhibitors: the chemistry and biological activity of U0126, its analogs, and cyclization products. Bioorg Med Chem Lett. 1998; 8(20):2839–2844. [PubMed: 9873633]

Fong A, Garcia E, Gwynn L, Lisanti MP, Fazzari MJ, Li M. Expression of caveolin-1 and caveolin-2 in urothelial carcinoma of the urinary bladder correlates with tumor grade and squamous differentiation. Am J Clin Pathol. 2003; 120:93–100. [PubMed: 12866378]

Frazier HA, Robertson JE, Dodge RK, Paulson DF. The value of pathologic factors in predicting cancer-specific survival among patients treated with radical cystectomy for transitional cell carcinoma of the bladder and prostate. Cancer. 1993; 71:3993–4001. [PubMed: 8508365]

Garrett SH, Somji S, Sens DA, Zhang KK. Prediction of the number of activated genes in multiple independent Cd(+2)-and As(+3)-indiced malignant transformations of human urothelial cells (UROtsa). PLoS One. 2014 Jan 22.9(1):e85614. [PubMed: 24465620]

Gerlinger M, Rowan AJ, Horswell S, Larkin J, Endesfelder D, Gronroos E, Martinez P, Matthews N, Stewart A, Tarpey P, Varela I, Phillimore B, Begum S, McDonald NQ, Butler A, Jones D, Raine K, Latimer C, Santos CR, Nohadani M, Eklund AC, Spencer-Dene B, Clark G, Pickering L, Stamp G, Gore M, Szallasi Z, Downward J, Futreal PA, Swanton C. Intratumor heterogeneity and branched evolution revealed by multiregion sequencing. N Engl J Med. 2012; 366:883–92. [PubMed: 22397650]

Gerlinger M, Catto JW, Orntoft TF, Real FX, Zwarthoff EC, Swanton C. Intratumour heterogeneity in urologic cancers: from molecular evidence to clinical implications. Eur Urol. 2015; 67:729–737. [PubMed: 24836153]

Hayashi T, Sentani K, Oue N, Anami K, Sakamoto N, Ohara S, Teishima J, Noguchi T, Nakayama H, Taniyama K, Matsubara A, Yasui W. Desmocollin 2 is a new immunohistochemical marker indicative of squamous differentiation in urothelia carcinoma. Histopathol. 2011; 59:710–721.

Huang W, Williamson SR, Rao Q, Lopez-Beltran A, Montironi R, Elbe JN, Grignon DJ, Idrees MT, Emerson RE, Zhou XJ, Zhang S, Baldridge LA, Hahn NM, Wang M, Koch MO, Cheng L. Novel markers of squamous differentiation in the urinary bladder. Human Pathol. 2013; 44:1989–1997. [PubMed: 23806524]

Izumi K, Zheng Y, Li Y, Zaengle J, Miyamoto H. Epidermal growth factor induces bladder cancer cell proliferation through activation of the androgen receptor. Int J Oncol. 2012; 41:1587–1592. [PubMed: 22922989]

Joo D, Woo JS, Cho KH, Han SH, Min TS, Yang DC, Yun CH. Biphasic activation of extracellular signal-regulated kinase (ERK) 1/2 in epidermal growth factor (EGF)-stimulated SW480 colorectal cancer cells. BMB Rep. 2016; 49:220–225. [PubMed: 26879318]

Kim SP, Frank I, Cheville JC, Thompson RH, Weight CJ, Thapa P, Boorjian SA. The impact of squamous and glandular differentiation on survival after radical cystectomy for urothelial carcinoma. J Urol. 2012; 188:405–409. [PubMed: 22704101]

Kyriakis JM, Avruch J. Mammalian Mitogen-Activated Protein Kinase Signal Transduction Pathways Activated by Stress and Inflammation. Physiological Reviews. 2001; 81:807–869. [PubMed: 11274345]

Logothetis CJ, Dexeus FH, Chong C, Sella A, Ayala AG, Ro JY, Pilat S. Cisplatin, cyclophosphamide and doxorubicin chemotherapy for unresectable urothelial tumors: the MD Anderson experience. J Urol. 1989; 41:33–37.

Lopez-Beltran A, Requena MJ, Alvarez-Kindelan J, Quintero A, Blanca A, Montironi R. Squamous differentiation in primary urothelial carcinoma of the urinary tract as seen by MAC387 immunohistochemistry. J Clin Pathol. 2009; 60:332–335.

Luke C, Tracey E, Stapleton A, Roder D. Exploring contrary trends in bladder cancer incidence, mortality and survival: implications for research and cancer control. Intern Med J. 2010; 40:357–362. [PubMed: 19460053]

Luster MI, Simeonova PP. Arsenic and urinary bladder cell proliferation. Toxicol Appl Pharmacol. 2004; 198:419–423. [PubMed: 15276422]

Ma S, Rao L, Freedberg IM, Blumenberg M. Transcriptional control of K5, K6, K14, and K17 keratin genes by AP-1 and NF-kappaB family members. Gene Expr. 1997; 6(6):361–370. [PubMed: 9495317]

MacLane NJ, Wood MD, Holder JC, Rees RW, Southgate J. Sensitivity of normal, premalignant, and malignant human urothelial cells to inhibitors of epidermal growth factor receptor signaling pathway. Mol Cancer Res. 2008; 6:53–63. [PubMed: 18234962]

Martin JE, Jenkins BJ, Zuk RJ, Blandy JP, Baithun SI. Clinical importance of squamous metaplasia in invasive transitional cell carcinoma of the bladder. J Clin Pathol. 1989; 42:250–253. [PubMed: 2703540]

Mellon K, Wright C, Kelly P, Horne CH, Neal DE. Long-term outcome related to epidermal growth factor receptor status in bladder cancer. J Urol. 1995; 153:919–925. [PubMed: 7853575]

Messing E, Gee JR, Saltzstein DR, Kim K, diSant'Agnese A, Kolesar J, Harris L, Faerber A, Havighurst T, Young JM, Efros M, Getzenberg RH, Wheeler MA, Tangrea J, Parnes H, House M, Busby JE, Hohl R, Bailey H. A phase 2 cancer chemoprevention biomarker trial of isoflavone G-2535 (genistein) in presurgical bladder cancer patients. Cancer Prev Res. 2012; 5:621–630.

Mitra AP, Bartsch CC, Bartsch G Jr, Miranda G, Skinner EC, Daneshmand S. Does presence of squamous and glandular differentiation in urothelial carcinoma of the bladder at cystectomy portend poor prognosis? An intensive case-control analysis. Urol Oncol. 2014; 32:117–127. [PubMed: 23477878]

Miyamoto H, Kubota Y, Noguchi S, Takase K, Matsuzaki J, Moriyama M, Takebayashi S, Kitamura H, Hosaka M. c-erbB-2 gene amplification as a prognostic marker in human bladder cancer. Urology. 2000; 55:679–683. [PubMed: 10792078]

Moll R, Divo M, Langbein L. The human keratins: biology and pathology. Histochem Cell Biol. 2008; 129:705–733. [PubMed: 18461349]

Mooso BA, Vinall RL, Mudryj M, Yap SA, White RW, Ghosh PM. The role of EGFR family inhibitions in muscle invasive bladder cancer: A review of clinical data and molecular evidence. J Urol. 2015; 193:19–29. [PubMed: 25158272]

Neal DE, Sharples L, Smith K, Fennelly J, Hall RR, Harris A. The epidermal growth factor receptor and the prognosis of bladder cancer. Cancer. 1990; 65:1619–1625. [PubMed: 2311071]

Perou CM, Sørlie T, Eisen MB, van de Rijn M, Jeffrey SS, Rees CA, Pollack JR, Ross DT, Johnsen H, Akslen LA, Fluge O, Pergamenschikov A, Williams C, Zhu SX, Lønning PE, Børresen-Dale AL, Brown PO, Botstein D. Molecular portraits of human breast tumors. Nature. 2000; 406:747–752. [PubMed: 10963602]

Rossi MR, Masters JRW, Park S, Todd JH, Garrett SH, Sens MA, Somji S, Nath J, Sens DA. The immortalized UROtsa cell line as a potential cell culture model of human urothelium. Environ Health Perspect. 2001; 109:801–808. [PubMed: 11564615]

Sens DA, Park S, Gurel V, Sens MA, Garrett SH, Somji S. Inorganic cadmium- and arsenite-induced malignant transformation of human bladder urothelial cells. Toxicol Sci. 2004; 79:56–63. [PubMed: 14976345]

Siegel R, Naishadham D, Jemal A. Cancer Statistics, 2013. CA Cancer J Clin. 2013; 63:11–30. [PubMed: 23335087]

Smith AH, Goycolea M, Haque R, Biggs ML. Marked increase in bladder and lung cancer mortality in a region of Northern Chile due to arsenic in drinking water. Am J Epidemiol. 1998; 147:660–669. [PubMed: 9554605]

Somji S, Bathula CS, Zhou XD, Sens MA, Sens DA, Garrett SH. Transformation of human urothelial cells (UROtsa) by As^{+3} and Cd^{+2} induces the expression of keratin 6a. Environ Health Perspect. 2008; 116:434–440. [PubMed: 18414623]

Somji S, Cao L, Mehus A, Zhou XD, Sens MA, Dunlevy JR, Garrett SH, Zheng Y, Larson JL, Sens DA. Comparison of expression patterns of keratin 6, 7, 16, 17 and 19 in bladder cancer. Cell Biol Toxicol. 2011; 27:381–396. [PubMed: 21927821]

Steinmaus C, Moore L, Hopenhayn-Rich C, Biggs ML, Smith AH. Arsenic in drinking water and bladder cancer. Cancer Invest. 2000; 18:174–182. [PubMed: 10705880]

Tsuda T, Babazono A, Yamamoto E, Kurumatini N, Mino Y, Ogawa T, Kishi Y, Aoyama H. Ingested arsenic and internal cancer: a historical cohort study followed for 33 years. Am J Epidemiol. 1995; 141:198–209. [PubMed: 7840093]

Zuiverloon TC, Nieuweboer AJ, Vekony H, Kirkels WJ, Bangma CH, Zwartoff EC. Markers predicting response to bacillus Calmette-Guerin immunotherapy in high-risk bladder cancer patients: a systematic review. Eur Urol. 2012; 61:128–145. [PubMed: 22000498]

Highlights

- Keratin 6 is induced in As^{+3}-transformed transformed UROtsa cells by EGF.
- The ERK1/2 signaling pathway regulates the expression of KRT6.
- As^{+3}-transformed human urothelial cells can serve as a model to study urothelial carcinomas.

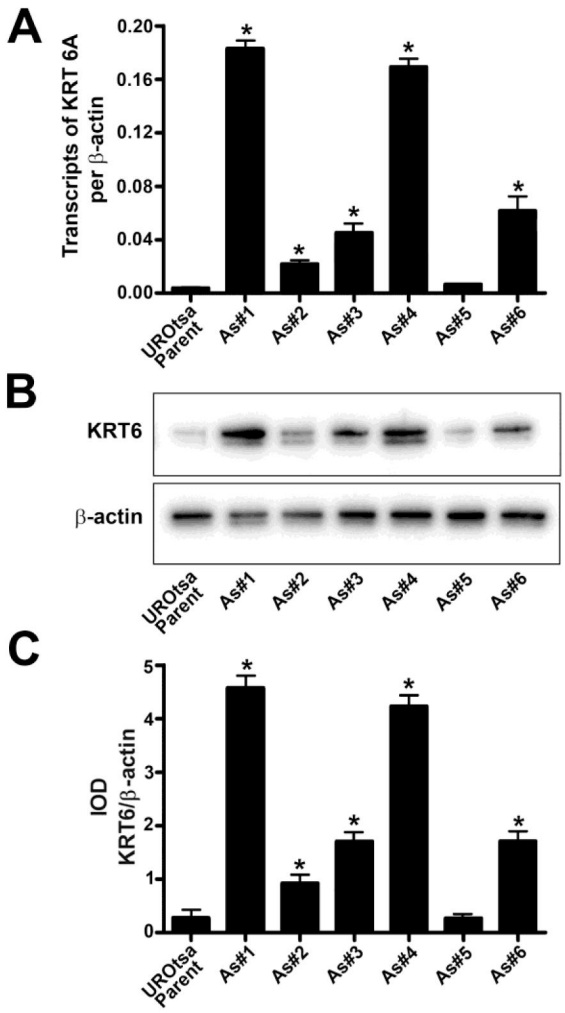

Fig. 1.

Expression of KRT6 in UROtsa parent cells and the As^{+3}-transformed UROtsa cells. (A). Real-time PCR analysis of KRT6a expression in UROtsa parent and As^{+3}-transformed UROtsa cells. The data is expressed as transcripts of KRT6 per transcript of β-actin. (B and C). Western blot analysis of KRT6 expression in UROtsa parent and As^{+3}-transformed UROtsa cells. The integrated optical densities (IOD) for each of the KRT6 band/β-actin is indicated. * indicates significantly different at $p<0.05$ from parent UROtsa cells.

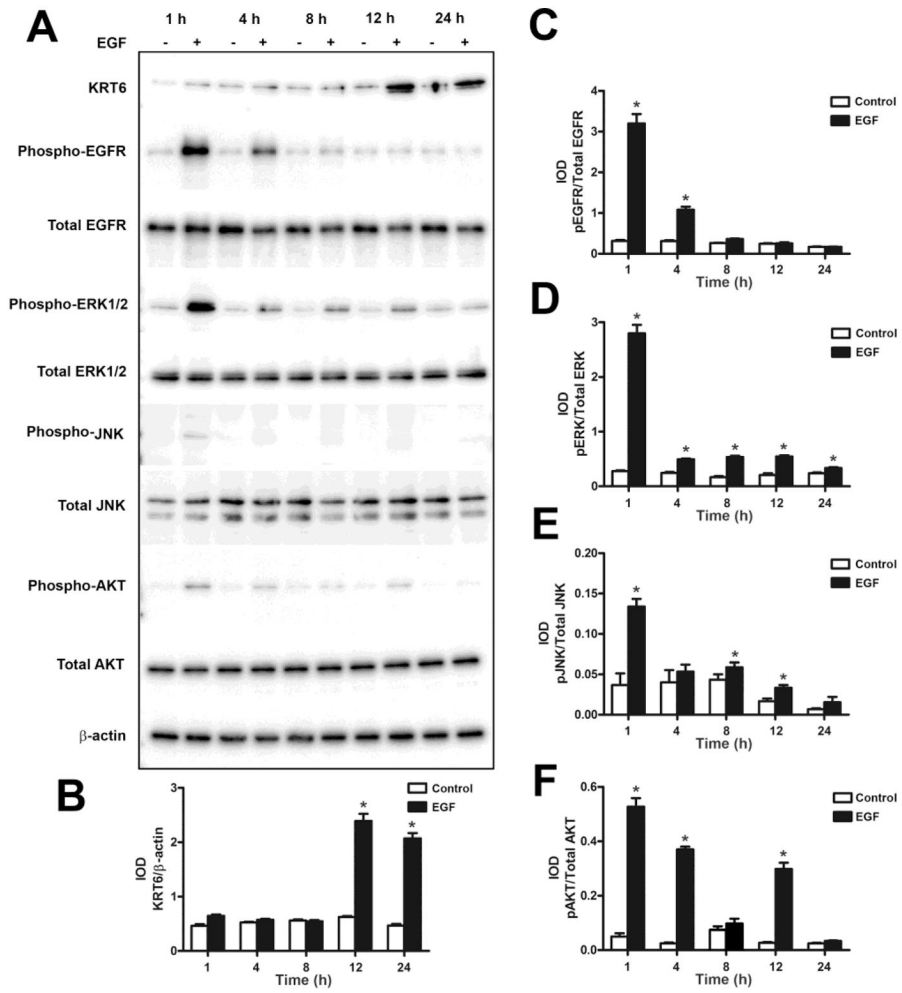

Fig. 2.

Effect of EGF on the expression of KRT6 and the activation of EGFR and downstream kinases in the UROtsa parent cells. (A and B). Western blot analysis of KRT6 expression in UROtsa parent cells after treatment with EGF for various time periods. The integrated optical densities (IOD) for each of the KRT6 band/β-actin is indicated. (A – F). Phosphorylation of EGFR (A and C), ERK1/2 (A and D), JNK (A and E) and AKT (A and F) was determined by Western blotting. The IOD for each phosphorylated protein is plotted per total protein. * indicates significantly different at $p<0.05$ from untreated controls for each time point.

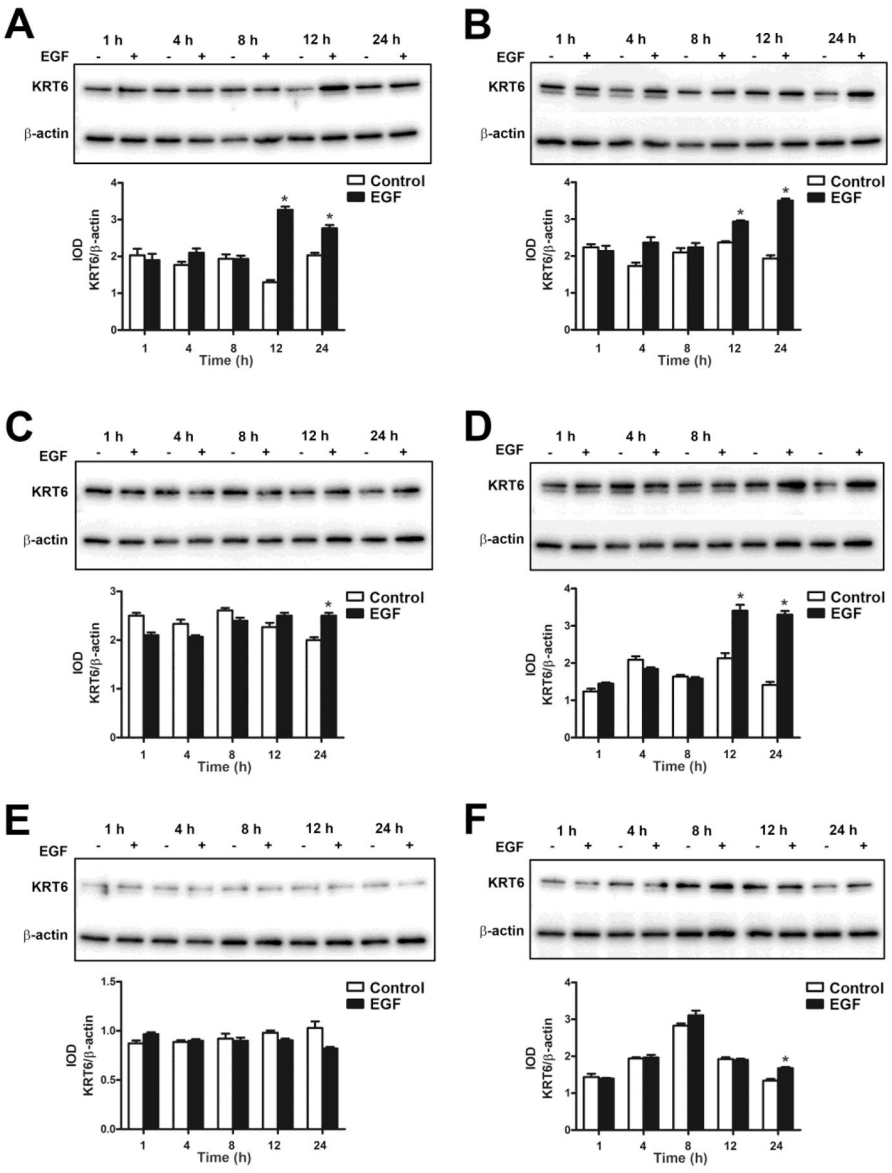

Fig. 3.

Effect of EGF on the expression of KRT6 in As^{+3}-transformed UROtsa cells. (A – F). Western blot analysis of KRT6 expression in As#1 (A), As#2 (B), As#3 (C), As#4 (D), As#5 (E) and As#6 (F) cells. The integrated optical densities (IOD) for each of the KRT6 band/β-actin is indicated. * indicates significantly different at $p<0.05$ from untreated controls for each time point.

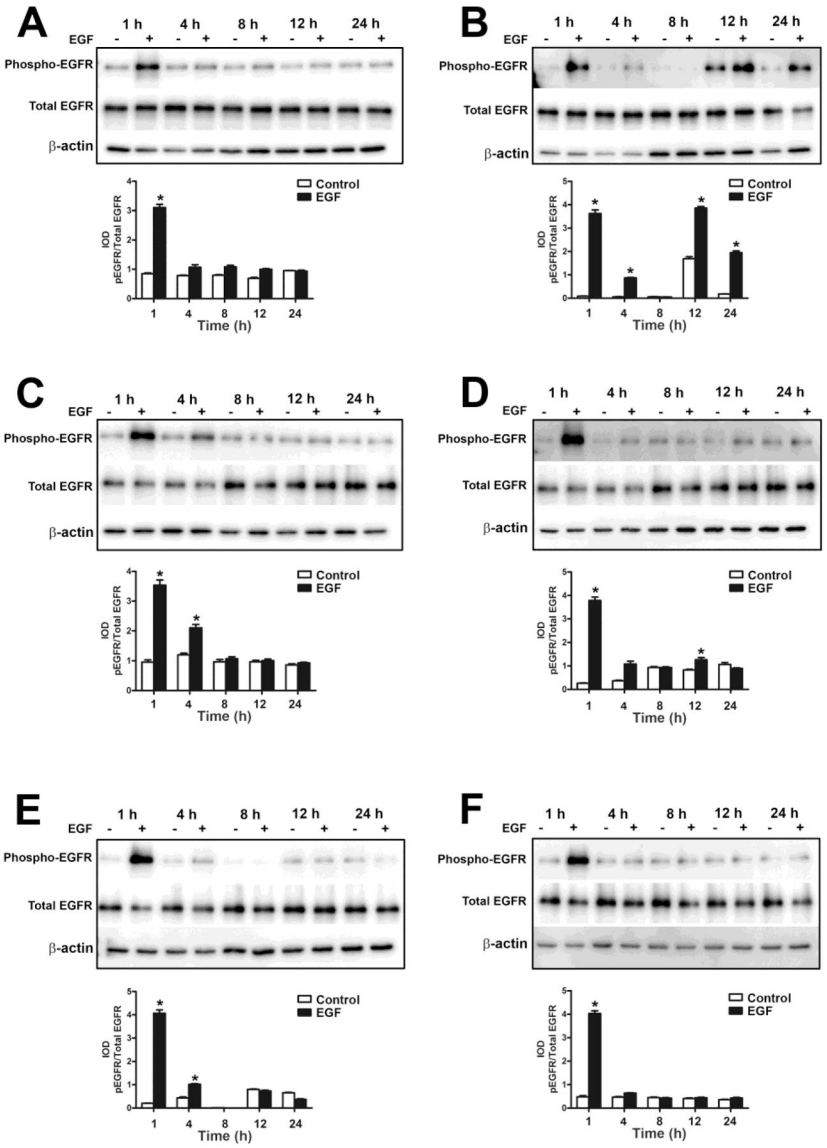

Fig. 4.

Effect of EGF on the phosphorylation of EGFR in As^{+3}-transformed UROtsa cells. Western blot analysis of phosphorylation of EGFR in As#1 (A), As#2 (B), As#3 (C), As#4 (D), As#5 (E) and As#6 (F) cells. The IOD for phosphorylated EGFR is plotted per total EGFR. * indicates significantly different at $p<0.05$ from untreated controls for each time point.

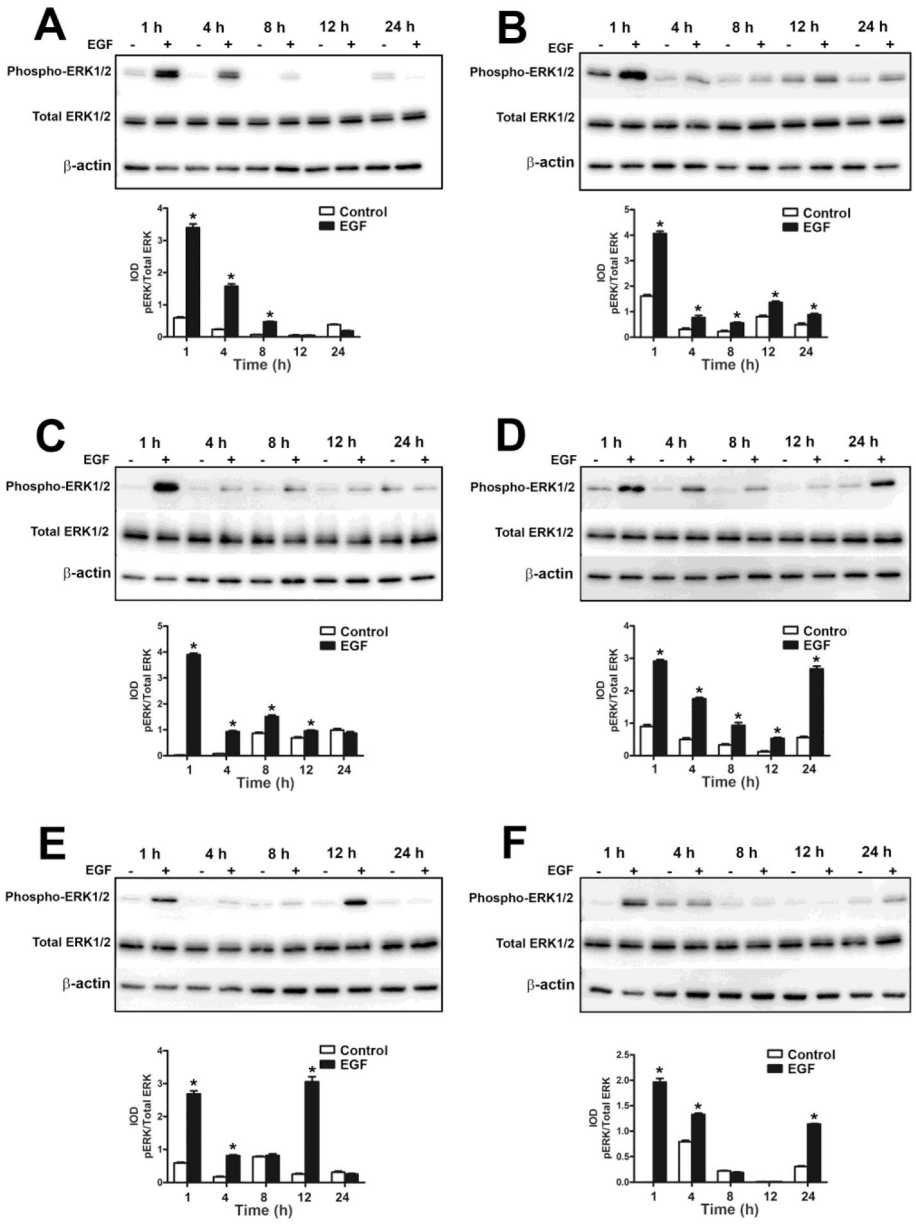

Fig. 5.

Effect of EGF on the activation of ERK1/2 in As^{+3}-transformed UROtsa cells. Western blot analysis of phosphorylation of ERK1/2 in As#1 (A), As#2 (B), As#3 (C), As#4 (D), As#5 (E) and As#6 (F) cells. The IOD for phosphorylated ERK1/2 is plotted per total ERK1/2. * indicates significantly different at $p<0.05$ from untreated controls for each time point.

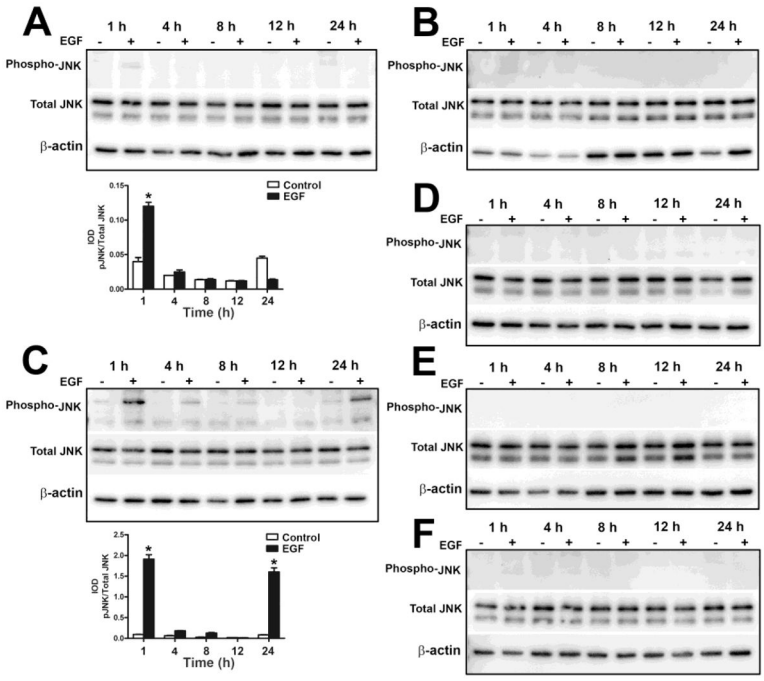

Fig. 6.

Effect of EGF on the activation of JNK in As^{+3}-transformed UROtsa cells. Western blot analysis of phosphorylation of JNK in As#1 (A), As#2 (B), As#3 (C), As#4 (D), As#5 (E) and As#6 (F) cells. The IOD for phosphorylated JNK is plotted per total JNK. * indicates significantly different at $p<0.05$ from untreated controls for each time point.

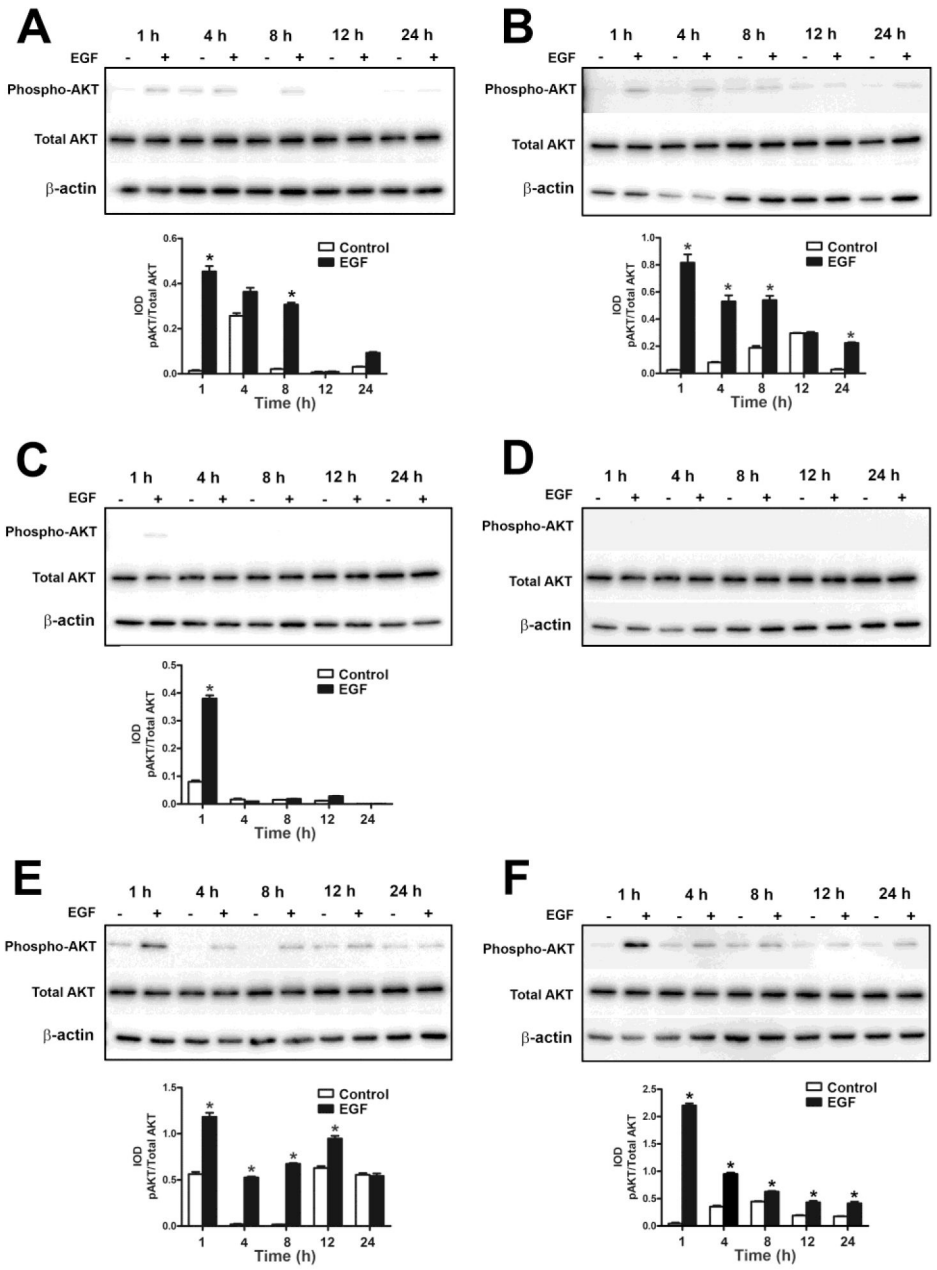

Fig. 7.

Effect of EGF on the activation of AKT in As^{+3}-transformed UROtsa cells. Western blot analysis of phosphorylation of AKT in As#1 (A), As#2 (B), As#3 (C), As#4 (D), As#5 (E) and As#6 (F) cells. The IOD for phosphorylated AKT is plotted per total AKT. * indicates significantly different at $p<0.05$ from untreated controls for each time point.

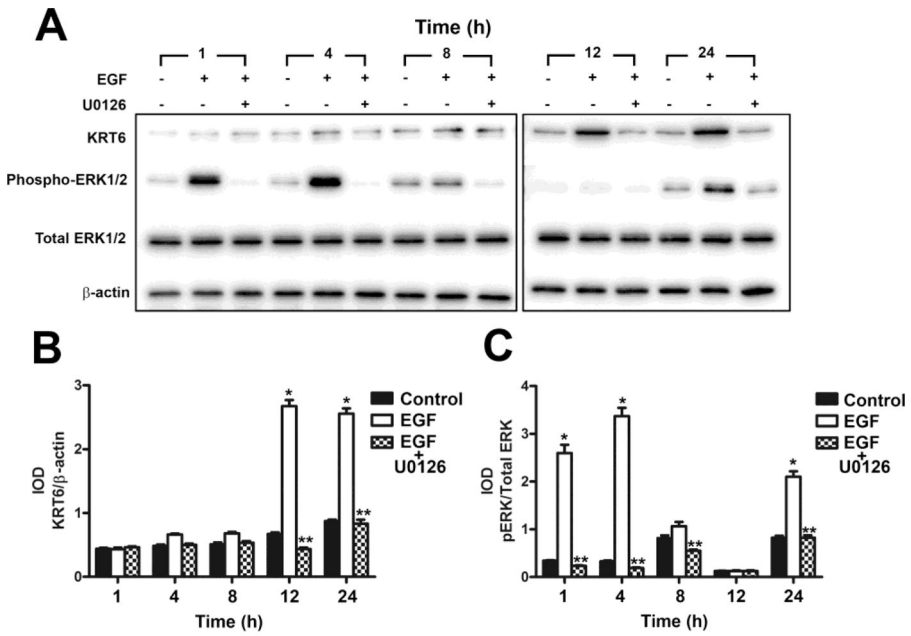

Fig. 8.

Effect of MEK1/2 inhibitor U0126 on the expression of KRT6 in UROtsa parent cells. (A and B). Western blot analysis of KRT6 expression in UROtsa cells treated with the MEK1/2 inhibitor U0126. The IOD for each of the KRT6 band/β-actin is indicated. (A and C). Western blot analysis of phosphorylation of ERK1/2 in UROtsa cells treated with the MEK1/2 inhibitor U0126. The IOD for phosphorylated ERK1/2 is plotted per total ERK1/2. * indicates significantly increased at $p<0.05$ from untreated controls for each time point. ** indicates significantly decreased from EGF only treated cells at $p<0.05$ for each time point.

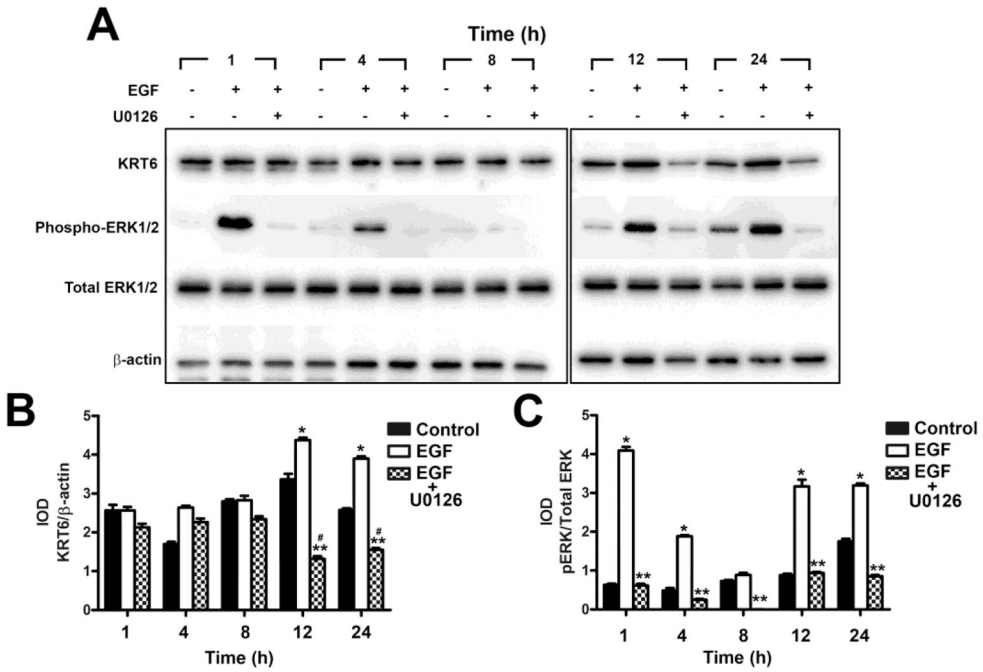

Fig. 9.

Effect of MEK1/2 inhibitor U0126 on the expression of KRT6 in As^{+3}-transformed UROtsa cells. (A and B). Western analysis of KRT6 expression in UROtsa cells treated with the MEK1/2 inhibitor U0126. The IOD for each of the KRT6 band/β-actin is indicated. (A and C). Western analysis of phosphorylation of ERK1/2 in As^{+3}-transformed UROtsa cells treated with the MEK1/2 inhibitor U0126. The IOD for phosphorylated ERK1/2 is plotted per total ERK1/2. * indicates significantly increased at $p<0.05$ from untreated controls for each time point. ** indicates significantly decreased from EGF only treated cells at $p<0.05$ for each time point. # indicates significantly decreased from untreated controls at $p<0.05$ for each time point.

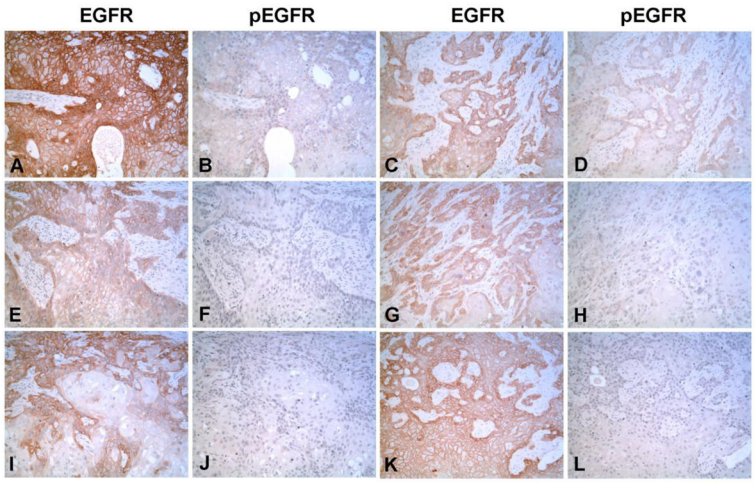

Fig. 10.

Immunohistochemical staining of EGFR and pEGFR in As^{+3}-transformed subcutaneous tumor heterotransplants. (A, C, E, G, I and K). Staining for EGFR in the As^{+3}-transformed cell line As#1, As#2, As#3, As#4, As#5 and As#6 respectively. B, D, F, H, J and L. Staining for pEGFR in As#1, As#2, As#3, As#4, As#5 and As#6 respectively. The staining is localized to the cell membrane for both EGFR and pEGFR and is most intense at the periphery of the tumor nests and less intense or absent in the center of the nests All micrographs are at x100 magnification.

Table 1

Immunostaining of EGFR and pEGFR in tumor heterotransplants

Group	EGFR		P-EGFR	
	Intensity	Percentage	Intensity	Percentage
As#1	3+	50%	1+	15%
As#2	2–3+	40%	1–2+	10%
As#3	2–3+	30%	-	0
As#4	2–3+	50%	-	0
As#5	3+	30%	-	0
As#6	3+	60%	-	0